

Mobile Sensor Networks: A New Approach for Structural Health Monitoring

Dapeng Zhu ¹, Xiaohua Yi ¹, Yang Wang ¹, Jiajie Guo ², Kok-Meng Lee ²

¹ School of Civil and Environmental Engineering, Georgia Institute of Technology,
Atlanta, GA 30332

² School of Mechanical Engineering, Georgia Institute of Technology, Atlanta, GA 30332

ABSTRACT

In this paper, a new approach using mobile sensor networks is proposed for structural health monitoring. Compared with static sensors, mobile sensor networks offer flexible system architectures with adaptive spatial resolutions. The paper describes the design concept of a flexure-based mechatronic (flexonic) mobile sensing node and its application in structural health monitoring. The flexonic mobile sensing node is capable of maneuvering on structures built with ferromagnetic materials, as well as attaching/detaching an accelerometer onto/from a steel structural surface. The performance of the prototype mobile sensor network has been validated through laboratory experiments, where two flexonic mobile sensing nodes are adopted for maneuvering on a steel portal frame. Transmissibility function analysis is then conducted to identify structural damage using data collected by the mobile sensing nodes. This preliminary work is expected to spawn transformative changes of using mobile sensors for future structural health monitoring.

INTRODUCTION

As civil structures are continuously subjected to adverse operational and environmental conditions, their safety condition becomes increasingly concerning over time. For example, more than one fourth of the bridges in the United States were categorized as structurally deficient or functionally obsolete, and it was estimated that a \$17 billion annual investment is needed to substantially improve current bridge conditions, yet currently, only \$10.5 billion is available annually for the construction and maintenance of bridges (ASCE 2009).

In order to efficiently utilize available resources and prioritize retrofit tasks, accurate evaluation of bridge conditions is essential. In recent years, significant research efforts have been devoted to structural health monitoring (SHM) systems that are promising in closely monitoring structural safety conditions. For example, the high cost of traditional cable-based structural monitoring systems motivated exploration in wireless sensing technologies that are free from expensive cable installation. To date, various academic and industrial wireless sensing prototypes have been developed and validated for structural health monitoring (Lynch and Loh 2006). As a transformative advancement to wireless sensing, the next revolution in sensor networks is predicted to be mobile sensing systems that contain individual mobile sensing nodes (Akyildiz *et al.* 2002). Each

mobile sensing node can explore its surrounding and exchange information with its peers by wireless communication. Compared with static wireless sensors, mobile sensor networks offer flexible system architectures with adaptive spatial resolutions.

Many efforts have been made in terms of incorporating mobility into traditional sensors. For example, a beam-crawler has been developed for wirelessly powering and interrogating battery-less peak-strain sensors; the crawler moves along the flange of an I-beam by wheels (Huston *et al.* 2001). In order to inspect the inner casing of ferromagnetic pipes, a compact robot with two magnetic wheels in a motorbike arrangement has been developed; the robot can slightly lift off the wheel in order to negotiate concave edges (Tache *et al.* 2009). Most recently, Lee *et al.* (2009) developed a flexure-based mechatronic (flexonic) mobile sensing node, which is capable of attaching/detaching an accelerometer onto/from the structural surface. Meanwhile, this flexonic mobile sensing node has the potential to fulfill functions of negotiating in complex steel structures with narrow sections and high abrupt angle changes. As a continuing effort, Guo *et al.* (2009) conducted further analysis on the compliant mechanism of the flexonic mobile sensing node.

In recent years, a myriad of vibration-based damage detection methods have been developed (Doebling *et al.* 1998). Among these methods, transmissibility function analysis has attracted significant interest due to its effectiveness in damage detection without requiring excitation force record. For example, Zhang *et al.* (1999) used translational and curvature transmissibility functions to calculate damage indicators and successfully located the damage on a cantilever beam. Their experimental results showed that the performance of damage localization varies with the frequency range adopted in the transmissibility function analysis. Other different aspects that may affect transmissibility function analysis have been explored, such as the linearity of structures (Johnson *et al.* 2004), the nature of input forces (Devriendt and Guillaume 2008), as well as the operational and environmental variability effects (Kess and Adams 2007). Based upon previous work, transmissibility function analysis is well understood, and is being widely investigated in dynamic experiments.

In another work, Yi *et al.* (2010) validate that the flexonic mobile sensing nodes are capable of detecting simulated structural damage through transmissibility function analysis. A steel mass block is bonded to a steel portal frame to simulate a reversible damage, which is not a common damage scenario occurring in actual civil structures. In this paper, a more realistic damage scenario with loosened bolts is adopted to validate the performance of the flexonic mobile sensing nodes. The paper begins with the design and implementation of the flexonic mobile sensing nodes. The formulation of transmissibility function analysis is then briefly introduced. Next, the setup of a laboratory validation experiment is presented and followed by the damage detection results using the data collected by the flexonic mobile sensing nodes. Finally, the paper concludes with a summary and a plan for future work.

IMPLEMENTATION OF A FLEXONIC MOBILE SENSING NODE

Figure 1 and Figure 2 show the flexonic mobile sensing node developed by Lee *et al.* (2009). This mobile sensing node consists of three substructures: two 2-wheel cars and a compliant connection beam. Each 2-wheel car contains a body frame, two

motorized wheels, batteries, a wireless sensing unit developed by Wang *et al.* (2007), as well as Hall-effect sensors and infrared (IR) sensors. The wheels of the flexonic mobile sensing node are surrounded by thin rectangular magnets so that they provide enough attraction force for the mobile sensing node to maneuver on ferromagnetic structures. The compliant connection beam between the two cars is made of flexible spring steel, with an accelerometer (manufactured by Silicon Designs, Inc.) mounted at the middle of the beam. The compliant connection beam assists in attaching/detaching an accelerometer onto/from the steel structural surface. When a measurement is to be made, the two cars drive towards each other to buckle the compliant beam down to the surface. With the assistance of some small magnets fixed around the center of the beam, the accelerometer is attached firmly on the steel surface (Figure 2 (a)). After measurement, the two cars move in opposite directions to straighten the beam and lift the accelerometer away from the steel surface (Figure 2 (b)). The width of the flexonic mobile sensing node is about 0.152m (6 in), and the height is about 0.091m (3.6 in). When the sensor is attached to the structural surface, the length of the mobile sensing node is 0.191m (7.5 in). When the sensor is detached, the length of the node is 0.229 m (9 in). The overall weight of the mobile sensing node is about 1 kg (2.2 lbs), most of which is contributed by the magnet wheels, motors, and batteries.

The functions of the wireless sensing unit include sampling analog signals from various sensors, processing sensor data, wireless communication, as well as motor control. A Hall-effect sensor, which is capable of measuring the flux of a magnetic field, is placed

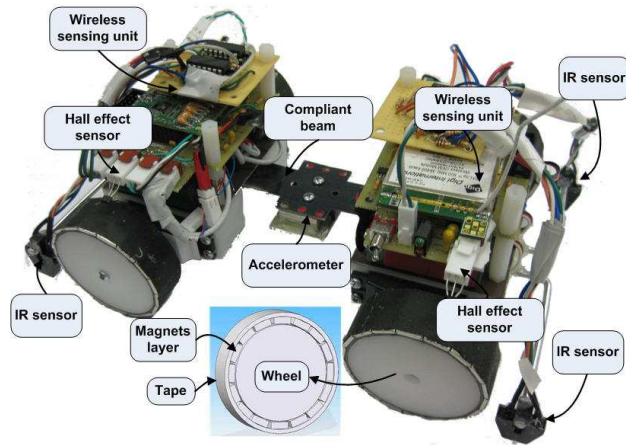


Figure 1. Picture of the flexonic mobile sensing node

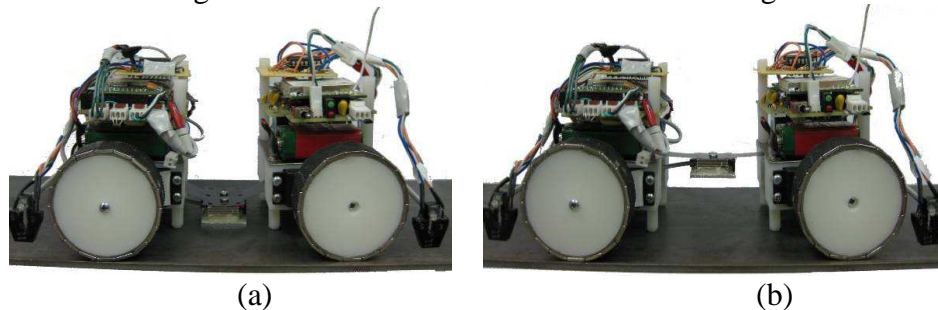


Figure 2. Side view of the flexonic magnet-wheeled mobile sensing node: (a) sensor attachment; (b) sensor detachment

above each magnet wheel. As the wheel rotates, the magnet flux density measured by the Hall-effect sensor changes periodically, so that the velocity of the wheel can be measured for feedback control. In order to move the mobile sensing node (both forward and backward) safely on the underlying structural surface, IR sensors are placed at both sides of the front 2-wheel car as well as the rear 2-wheel car for surface boundary detection. When the sensing node tends to move outside the surface boundary, changes can be captured in the reflected IR signal and the movement direction will be immediately corrected. Detailed description about the control of the flexonic mobile sensing node can be found in Lee *et al.* (2009).

OVERVIEW OF TRANSMISSIBILITY FUNCTION ANALYSIS

The equation of motion for an n -degree-of-freedom (n -DOF) linear structure under external excitation can be formulated as:

$$\mathbf{M}\ddot{\mathbf{x}}(t) + \mathbf{C}\dot{\mathbf{x}}(t) + \mathbf{K}\mathbf{x}(t) = \mathbf{f}(t) \quad (1)$$

where \mathbf{M} , \mathbf{C} , \mathbf{K} are $n \times n$ mass matrix, viscous damping matrix and stiffness matrix, respectively. $\mathbf{x}(t)$ is the $n \times 1$ displacement vector, and $\mathbf{f}(t)$ is the $n \times 1$ external input vector.

Using Fourier transform, the equation of motion can be represented in frequency domain as:

$$\mathbf{X}(\omega) = \mathbf{H}(\omega)\mathbf{F}(\omega) \quad (2)$$

where $\mathbf{H}(\omega) = (\mathbf{K} - \omega^2\mathbf{M} + i\omega\mathbf{C})^{-1}$ is the $n \times n$ frequency response function matrix. The acceleration vector in the frequency domain can be formulated as:

$$\mathbf{A}(\omega) = -\omega^2\mathbf{H}(\omega)\mathbf{F}(\omega) \quad (3)$$

Assuming the external force is only applied to the k -th DOF, the Fourier transform of the input force vector $\mathbf{f}(t)$ is described as:

$$\mathbf{F}(\omega) = \{0_1, 0_2, \dots, F_k(\omega), \dots, 0_N\}^T \quad (4)$$

Substituting Equation (4) into Equation (3), we get

$$\mathbf{A}(\omega) = -\omega^2 F_k(\omega) \mathbf{H}_k(\omega) \quad (5)$$

where $\mathbf{H}_k(\omega)$ is the k -th column of $\mathbf{H}(\omega)$.

The transmissibility function $T_{ij}(\omega)$ between the DOF i and reference-DOF j is defined as the ratio between the frequency responses at these two DOFs, $A_i(\omega)$ and $A_j(\omega)$.

$$T_{ij}(\omega) = \frac{A_i(\omega)}{A_j(\omega)} = \frac{-\omega^2 H_{ik}(\omega) F_k(\omega)}{-\omega^2 H_{jk}(\omega) F_k(\omega)} = \frac{H_{ik}(\omega)}{H_{jk}(\omega)} \quad (6)$$

On the other hand, the transmissibility function between DOF i and DOF j can also be expressed as

$$T_{ji}(\omega) = \frac{A_j(\omega)}{A_i(\omega)} = \frac{H_{jk}(\omega)}{H_{ik}(\omega)} \quad (7)$$

When the magnitude of $H_{jk}(\omega)$ is close to zero, the transmissibility function T_{ij} calculated by Equation (6) may encounter greater numerical error and therefore, more susceptible to noise in sensor data. In comparison, the transmissibility function T_{ji} calculated by Equation (7) may lose accuracy when the frequency response function $H_{ik}(\omega)$ has a small magnitude. Among $T_{ij}(\omega)$ and $T_{ji}(\omega)$, if one approach of calculating the transmissibility function is more susceptible to sensor noise, the other approach can be chosen to reduce the noise influence.

Based upon the transmissibility function $T_{ij}(\omega)$, an integral damage indicator (DI) between the DOF i and DOF j is defined as:

$$DI_{ij} = \int_{\omega_1}^{\omega_2} \frac{|\ln|T_{ij}^U| - \ln|T_{ij}^D||}{|\ln|T_{ij}^U||} d\omega \quad (8)$$

where superscript U and D represent the undamaged structure and the damaged structure, respectively, and “ln” means natural logarithm. Accordingly, T_{ij}^U and T_{ij}^D represent the transmissibility function of the undamaged structure and the damaged structure, respectively; ω_1 and ω_2 are the lower and upper boundaries of the interested frequency span. If the damage indicators between two DOFs are large, it is likely that structural damage has occurred around these two DOFs.

In order to reduce the effect of experimental uncertainties, the measurement at each configuration is repeated for N times for both the undamaged and damaged structures. The damage indicator is then calculated using the averaged transmissibility functions as following:

$$T_{ij}^U = \frac{1}{N} \sum_{k=1}^N (T_{ij}^U)_k \quad (9a)$$

$$T_{ij}^D = \frac{1}{N} \sum_{k=1}^N (T_{ij}^D)_k \quad (9b)$$

where the subscript k represents the k -th repeating test.

LABORATORY EXPERIMENTS

Experimental setup

Figure 3(a) shows a laboratory steel portal frame structure used for investigating structural damage detection using the flexonic mobile sensing nodes. The span of the portal frame is 1.524m (5 ft), and the height is 0.914m (3 ft). The beam and two columns have the same rectangular section area of 0.152m (6 in) \times 0.005m (3/16 in). Hinge connections are adopted at the bases of the two columns. Each column is connected with the beam through an angle plate, with 4 bolts on the beam and 4 bolts on the column. To simulate damage, the 4 bolts at the left corner of the beam are loosened. For the undamaged structure, the torque of each bolt is set at 13.56Nm (120 lbs-in); while for the damaged structure, the torque is reduced to 0.565Nm (5lbs-in), as shown in Figure 3(b) and Figure 4.

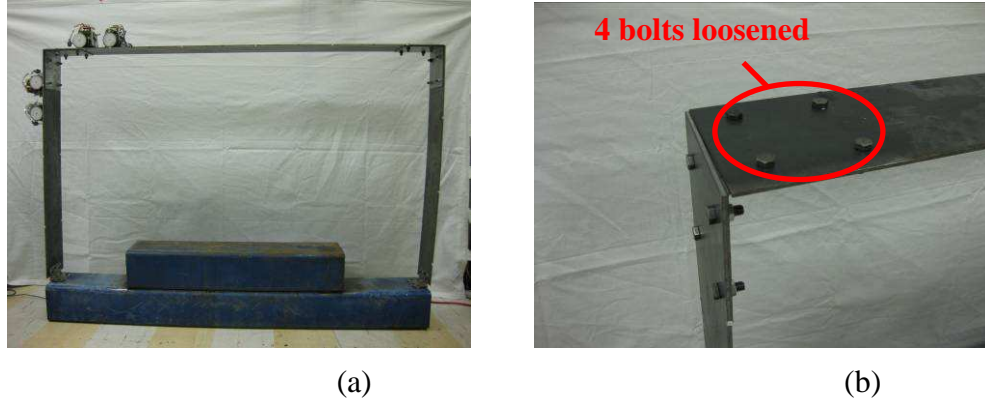


Figure 3. Photographs of the damage detection experiments: (a) picture of the portal frame with two mobile sensing nodes; (b) picture of the damage location with 4 bolts loosened.

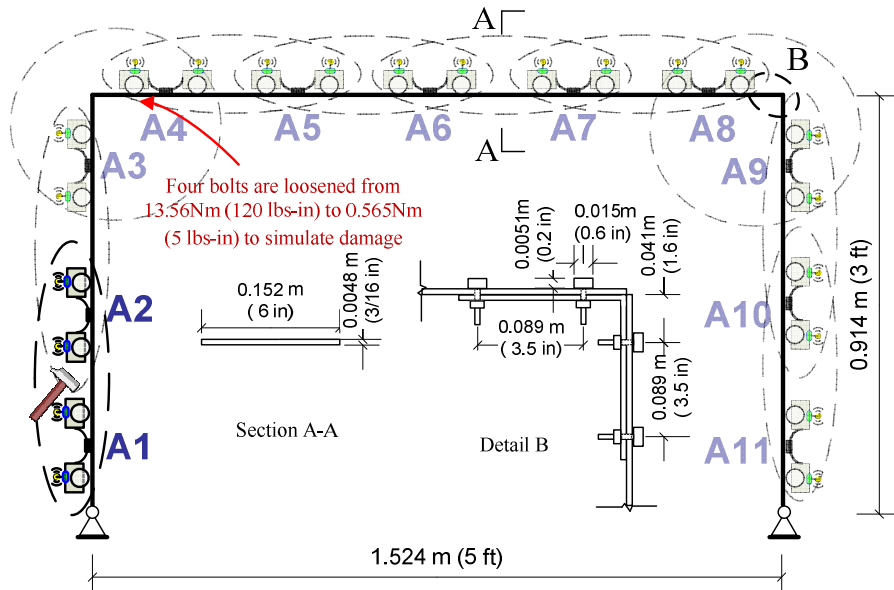


Figure 4. Experimental setup for damage detection using a steel portal frame

Two mobile sensing nodes are used in the experiments. Each mobile sensing node carries a Silicon Designs 2260-010 accelerometer. On both the undamaged structure and damaged structure, the two mobile sensing nodes move to every pair of locations to take acceleration measurements (A1-A2, A2-A3, A3-A4, A4-A5, A5-A6, A6-A7, A7-A8, A8-A9, A9-A10, and A10-A11). When the two mobile sensing nodes arrive at one pair of measurement locations, the accelerometer is attached onto the structural surface; then a hammer impact is applied at the middle of these two adjacent measurement locations, as illustrated in Figure 4. After the vibration measurement, these two mobile sensing nodes detach the accelerometers, and move to the next pair of measurement locations. In order to reduce the effect of experimental uncertainties, the measurement at each configuration is repeatedly taken for 20 times, i.e. $N = 20$ in Equation (9). The sampling rate for the acceleration measurement is set to 2500 Hz.

Transmissibility function analysis and damage detection results

Figure 5 compares the magnitude of the averaged transmissibility functions of the undamaged structure and the damaged structure. Note that the frequency range 100-1000 Hz is used, i.e. ω_1 and ω_2 in Equation (8) are set to 100Hz and 1000 Hz, respectively. Figure 5 shows that the transmissibility function at location A3 and A4 (T_{3-4}) has the largest difference between the damaged and undamaged structures, which corresponds to the correct damage location illustrated in Figure 4.

Besides comparing the transmissibility functions between the undamaged and damaged structures, the repeatability of the experiments is verified using the data sets from the undamaged structure, as well as from the damaged structure. Taking the damaged structure as an example, the 20 acceleration data sets collected at each pair of

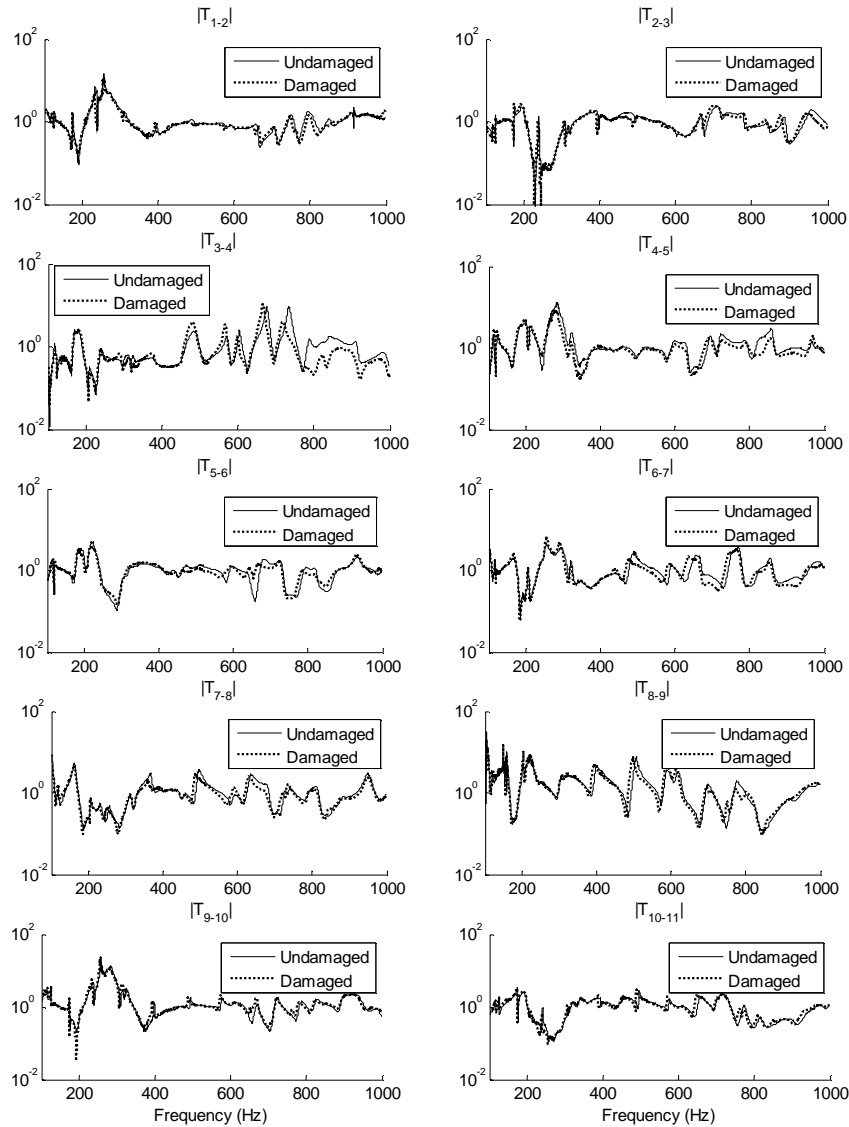


Figure 5. Comparison of averaged transmissibility functions between data sets of the undamaged and damaged structures.

locations are separated into two groups of 10 data sets. One group is constituted by the data sets with odd sequence numbers and the other group includes the data sets with even sequence numbers. Figure 6 compares the magnitude of the averaged transmissibility functions with the odd-sequence data group (T_{ij}^{odd}) and the even-sequence data group (T_{ij}^{even}) of the damaged structure. Minor differences exist between the transmissibility functions calculated from two groups of data sets, due to the inherent randomness of the laboratory experiments. However, the difference is much less than the difference between the transmissibility functions of the undamaged and damaged structures (shown in Figure 5), and is relatively negligible. Due to page limit, the comparison of transmissibility functions among the 20 data sets of the undamaged structure are not shown, and can be found in Yi *et al.* (2010).

The damage indicator defined in Equation (8) can be used to quantify the difference

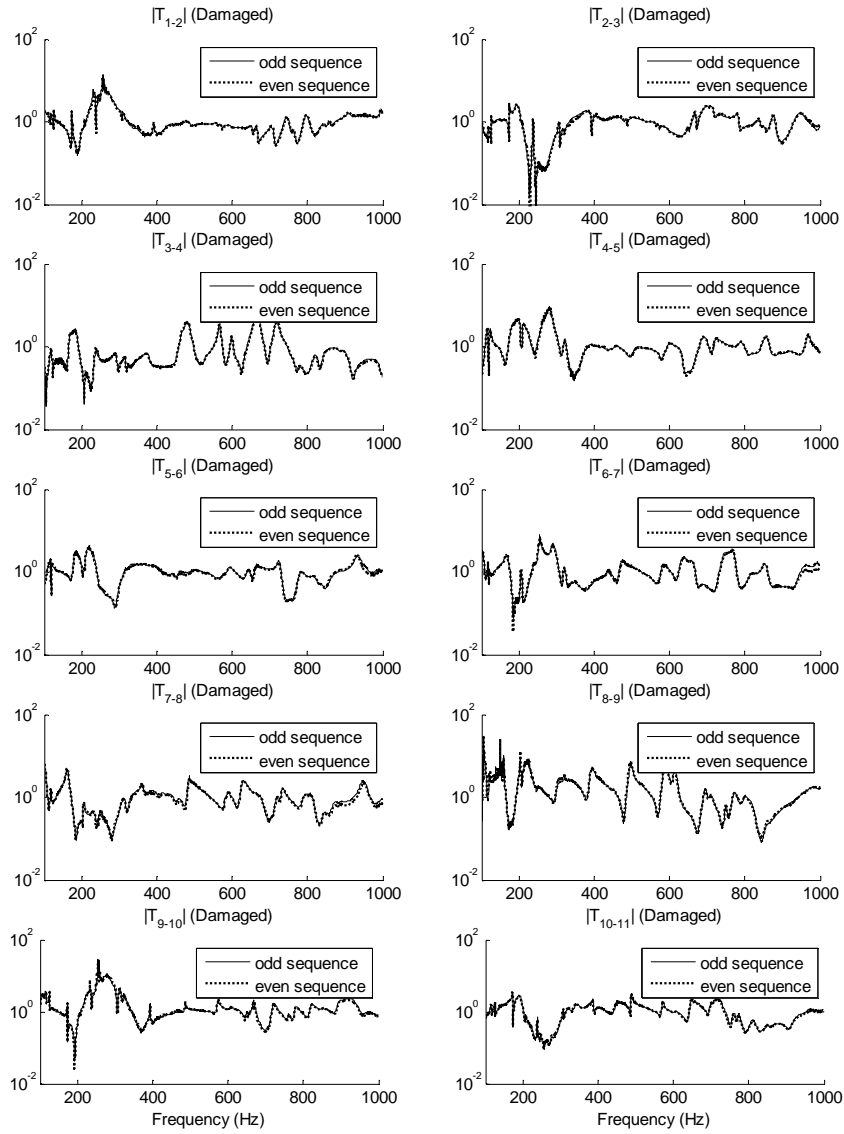


Figure 6. Comparison of the averaged transmissibility functions between odd-sequence data group and even-sequence data group of the damaged structure

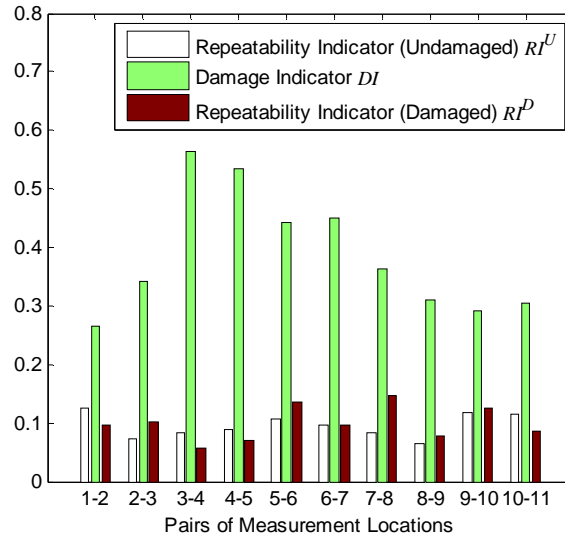


Figure 7. The damage indicators and repeatability indicators

between two groups of transmissibility functions. Figure 7 shows the damage indicators of the damaged structure. The largest damage indicator is $DI_{3-4} = 0.56$, and the location pair A3 and A4 is the correct damage location where bolts are loosened. In addition, by replacing T_{ij}^U and T_{ij}^D with T_{ij}^{odd} and T_{ij}^{even} in Equation (8), the repeatability indicators (RI) can be obtained for the undamaged structure, as well as for the damaged structure. Note that a smaller RI means a higher repeatability. As shown in Figure 7, all repeatability indicators of the experiments for the undamaged and damaged structure are close to 0.1. These small repeatability indicators verify that the experimental uncertainties have limited effects to damage detection results.

CONCLUSION AND FUTURE WORK

This work explores flexonic mobile sensor networks for structural health monitoring and damage detection. The presented flexonic mobile sensing nodes are capable of maneuvering upon steel structures, and are able to attach/detach an accelerometer onto/from the structural surface. Two flexonic mobile sensing nodes are used for vibration testing of a laboratory steel portal frame. With the acceleration data collected by the mobile sensors, transmissibility function analysis is conducted, and the damage location is successfully identified.

Future research will be conducted to enable the mobile sensing nodes to autonomously detect damage by embedding damage detection algorithms into the computational core of the mobile sensing nodes. In addition, a significant amount of efforts will be needed to improve the mobile sensing system for navigating on real-world structures built with ferromagnetic materials.

ACKNOWLEDGEMENT

This research is partially sponsored by the National Science Foundation, under grant number CMMI-0928095 (Program Manager: Dr. Shih-Chi Liu). The authors gratefully acknowledge the support.

REFERENCES

- Akyildiz, I. F., Su, W., Sankarasubramaniam, Y., and Cayirci, E. (2002). "A survey on sensor networks." *Communications Magazine, IEEE*, 40(8), 102-114.
- ASCE. (2009). *Report Card for America's Infrastructure*, American Society of Civil Engineers, Reston, VA.
- Devriendt, C., and Guillaume, P. (2008). "Identification of modal parameters from transmissibility measurements." *Journal of Sound and Vibration*, 314(1-2), 343-356.
- Doebling, S. W., Farrar, C. R., and Prime, M. B. (1998). "A summary review of vibration-based damage identification methods." *The Shock and Vibration Digest*, 30(2), 91-105.
- Guo, J., Lee, K.-M., Zhu, D., and Wang, Y. (2009). "A flexonic magnetic car for ferro-structural health monitoring." *Proceeding of 2009 ASME, Dynamic Systems and Control Conference*, Hollywood, CA. October 12-14, 2009.
- Huston, D. R., Esser, B., Gaida, G., Arms, S. W., and Townsend, C. P. (2001). "Wireless inspection of structures aided by robots." *Proceedings of SPIE, Health Monitoring and Management of Civil Infrastructure Systems*, Newport Beach, CA, 4337: 147-154. March 6, 2001.
- Johnson, T. J., Brown, R. L., Adams, D. E., and Schiefer, M. (2004). "Distributed structural health monitoring with a smart sensor array." *Mechanical Systems and Signal Processing*, 18(3), 555-572.
- Kess, H. R., and Adams, D. E. (2007). "Investigation of operational and environmental variability effects on damage detection algorithms in a woven composite plate." *Mechanical Systems and Signal Processing*, 21(6), 2394-2405.
- Lee, K.-M., Wang, Y., Zhu, D., Guo, J., and Yi, X. (2009). "Flexure-based mechatronic mobile sensors for structure damage detection." *Proceeding of the 7th International Workshop on Structural Health Monitoring*, Stanford, CA. September 9-11, 2009.
- Lynch, J. P., and Loh, K. J. (2006). "A summary review of wireless sensors and sensor networks for structural health monitoring." *The Shock and Vibration Digest*, 38(2), 91-128.
- Tache, F., Fischer, W., Caprari, G., Siegwart, R., Moser, R., and Mondada, F. (2009). "Magnebike: A magnetic wheeled robot with high mobility for inspecting complex-shaped structures." *Journal of Field Robotics*, 26(5), 453-476.
- Wang, Y., Lynch, J. P., and Law, K. H. (2007). "A wireless structural health monitoring system with multithreaded sensing devices: design and validation." *Structure and Infrastructure Engineering*, 3(2), 103-120.
- Yi, X., Zhu, D., Wang, Y., Guo, J., and Lee, K.-M. (2010). "Transmissibility-function-based structural damage detection with tetherless mobile sensors." *Proceeding of the Fifth International Conference on Bridge Maintenance, Safety and Management*, Philadelphia, Pennsylvania. July 11-15, 2010.
- Zhang, H., Schulz, M. J., Ferguson, F., and Pai, P. F. (1999). "Structural health monitoring using transmittance functions." *Mechanical Systems and Signal Processing*, 13(5), 765-787.